Uncovering the deep structure of the Koillismaa Layered Intrusion Complex, Finland using a novel 3D seismic survey

5 Michał Malinowski[1,2], Tuomo Karinen[1], Uula Autio[1], Suvi Heinonen[3], Brij Singh[2], Andrzej Górszczyk[2], Łukasz Sito[4], and the SEEMS DEEP Working Group*

[1]Geological Survey of Finland, Vuorimiehentie 5, 02151 Espoo, Finland
[2]Institute of Geophysics, Polish Academy of Sciences Warsaw, Księcia Janusza 64, 01-452 Warsaw, Poland
[3]Institute of Seismology, University of Helsinki, PO BOX 68 (Pietari Kalmin katu 5), Helsinki, Finland
10 [4]Geopartner Geofizyka Sp. z o.o., Skośna 39B, 30-383, Kraków, Poland
*A full list of authors appears at the end of the paper.

Correspondence to: Michal Malinowski (michal.malinowski@gtk.fi)

Abstract. A pioneering ~22 km² three-dimensional (3D) seismic survey was conducted in northeastern Finland within the SEEMS DEEP project to investigate the concealed Koillismaa Deep Intrusion (KDI), part of the 2.5–2.4 Ga Koillismaa–
15 Näränkävaara Layered Intrusion Complex (KLIC). Utilizing low-cost piezoelectric nimble nodes and a single Vibroseis source, this survey represents one of the first 3D seismic investigations of a deep layered intrusion and its feeder system. The seismic data, supported by petrophysical measurements and synthetic modelling, reveal a complex internal architecture characterized by coherent reflectivity patterns indicative of modal layering. Interpretation suggests that the KDI is not a simple feeder but a more developed, chonolithic or funnel-tube-shaped intrusion. Integration of seismic data interpretation with gravity inversion
20 and geological data enabled the construction of a Common Earth Model (CEM), which successfully reproduces the observed gravity anomaly. A major thrust fault, likely associated with the Oulujärvi Shear Zone, was imaged for the first time, offering new insights into the tectonic evolution and mineralization potential of the region. This study highlights the advances in 3D seismic methods in hardrock environment and establishes a methodological framework for future mineral exploration in similar geological settings.

1 Introduction

25 The application of seismic methods in mineral exploration within hardrock environments has gained considerable momentum in recent years (Malehmir et al., 2012b). This shift is largely driven by the increasing need to explore deeper and in more structurally complex geological settings, where traditional geophysical techniques (e.g., potential fields, various electromagnetic methods) often fall short. Three-dimensional (3D) seismic surveys have become indispensable for delivering 30 high-resolution images of the subsurface and for identifying potential drilling targets. Notable 3D seismic projects have been

conducted in Canada (Bellefleur et al., 2015; White et al., 2012), South Africa (Manzi et al., 2012), Finland (Malehmir et al., 2012a), Sweden (Malehmir et al., 2021), Portugal (Yavuz et al., 2015), and Australia (Schijns et al., 2023; Ziramov et al., 2023), demonstrating the effectiveness of this technology in generating direct exploration targets (White et al., 2016). Technological advances originally developed for the oil and gas industry - such as high-channel-count nodal sensors and

35   single-receiver, single-source acquisition - are now being successfully adapted for mineral exploration (Ziramov et al., 2023).

In this context, we present the results of a novel ~22 km² 3D seismic survey conducted in northeastern Finland as part of the SEEMS DEEP project (Autio et al., 2024), aimed at imaging the Koillismaa–Näränkävaara Layered Intrusion Complex (KLIC). Utilizing low-cost piezoelectric nimble nodes in a single-point configuration, this survey represents one of the first

40   3D seismic investigations of a layered intrusion and its feeder system at depths exceeding 1 km. The KLIC, part of the 2.5– 2.4 Ga mafic-ultramafic layered intrusions of the Fennoscandian Shield (Karinen, 2010), is globally recognized for its potential to host economically significant mineral deposits, including Ni-Cu-Co-PGE and V-Ti-Fe mineralization. The complex is expressed as a ~50 km long gravity anomaly, initially tested in 2020 by the Geological Survey of Finland (GTK) through a ~1.7 km deep drillhole, which intersected the intrusion at a depth of ~1.4 km (referred to as the Koillismaa Deep Intrusion,

45   KDI; Tirroniemi et al., 2024). Subsequent Distributed Acoustic Sensing (DAS) – Vertical Seismic Profiling (VSP) survey confirmed internal reflectivity within the KDI (Malinowski et al., 2023), validating the use of seismic methods for imaging the KLIC.

We begin by establishing the geological and petrophysical framework of the KLIC, utilizing the data from the Koillismaa deep

50   drillhole and representative stratigraphy from the exposed sections. We then describe the design, acquisition, and processing of the SEEMS DEEP 3D seismic survey. One of the highlights of this study is the successful use of 5D data interpolation to regularize the data prior to pre-stack time migration, contributing to improved migrated data quality. To our knowledge, this process was not extensively tested in case of hardrock seismic data. The resulting seismic volume, interpreted alongside synthetic modelling and gravity data, reveals a complex internal architecture of KDI and forms the basis for a new Common

55   Earth Model (CEM) of the region. Our findings challenge the long-standing interpretation of the KDI as a simple feeder system and support its reinterpretation as a more evolved, chonolithic or funnel-shaped layered intrusion. These results not only advance our understanding of the KLIC but also demonstrate the power of 3D seismic imaging in hardrock environments, with implications for tectonic reconstruction and mineral exploration.

2 Geological setting of the study area

60   The Fennoscandian Shield hosts numerous ~2.51–2.43 Ga mafic-ultramafic layered intrusions, formed during a major magmatic episode associated with the breakup of one or more Archaean cratons (Bleeker & Ernst, 2006; Ciborowski et al., 2015; Heaman, 1997; Köykkä et al., 2019; Skyttä et al., 2019). In Finland, most of these intrusions are located within the 2.44

Handwritten annotations (red):
- STRIDE nimble system
- proper reference to the acquisition system (a possibility is ref..1.)
- A reference to CEM would be good for the reader. perhaps 2)
- 2) McGaughey, John. "The common earth model: A revolution in mineral exploration data integration." GIS applications in the earth sciences 44 (2006): 567-576.
- 2) Mukerji, Biplab. "Modern techniques for identifying mineralization in virgin area." Innovative Exploration Methods for Minerals, Oil, Gas, and Groundwater for Sustainable Development. Elsevier, 2022. 297-309.
- 1) Amine Ourabah, Allan Chatenay; Unlocking ultra-high-density seismic for CCUS applications by combining nimble nodes and agile source technologies. The Leading Edge 2022;; 41 (1): 27–33. doi: https://doi.org/10.1190/tle41010027.1

Ga Tornio–Näränkävaara Belt (TNB; Alapieti & Lahtinen, 2002; Fig. 1a), a region of high economic interest due to known orthomagmatic PGE-Cu-Ni, V-Fe-Ti, and Cr mineralization. The TNB lies along the contact between the Archaean basement and the overlying Palaeoproterozoic greenstone and schist belts, extending from the Finnish–Swedish border to the Finnish–Russian border. The magmatism in the TNB, along with other 2.51–2.43 Ga intrusions in Fennoscandia, is now interpreted as part of an early rift-basin development episode, characterized by bimodal magmatism linked to the breakup of an Archaean supercontinent (Köykkä et al., 2019).

65
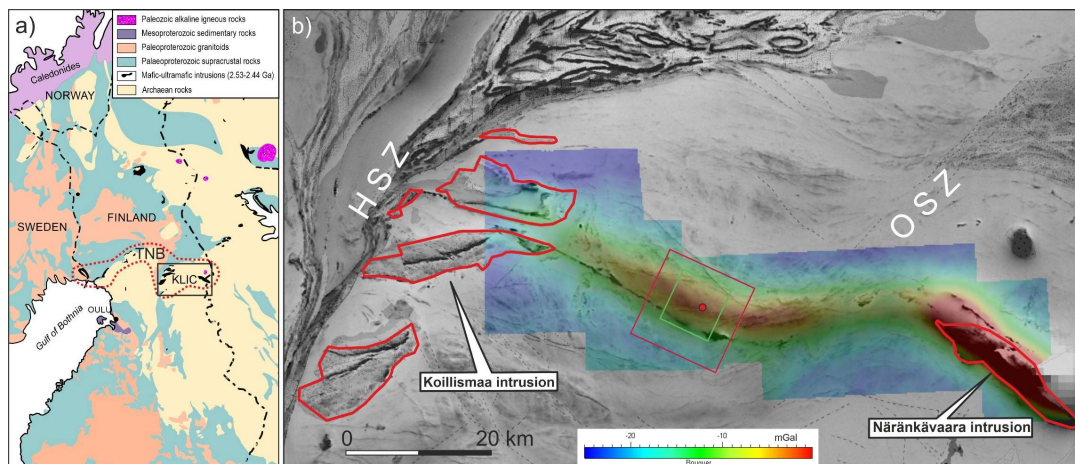
Figure 1: a) Simplified geological map of the Fennoscandian Shield (modified from Karinen 2010); KLIC = Koillismaa–Näränkävaara Layered Intrusion Complex, TNB = Tornio–Näränkävaara Belt; b) location of the study area with the composite image of the magnetic and Bouguer gravity anomaly maps. Red dot marks the Koillismaa drillhole, rectangles mark the extend of the SEEMS DEEP 3D seismic survey (green) and the Common Earth Model area (red); HSZ = Hirvaskoski Shear Zone, OSZ = Oulujärvi Shear Zone.

70

75

Our study area (Fig. 1b) is situated in the central part of the KLIC which is a component of the TNB (Fig. 1a). The KLIC comprises of two exposed intrusions — the Koillismaa Intrusion in the west and the Näränkävaara Intrusion in the east — connected by a ~50 km long geophysical anomaly (Alapieti, 1982; Karinen, 2010) (Fig. 1b). The Näränkävaara Intrusion, composed mainly of the ultramafic cumulates, is surrounded by the Archaean gneiss and has largely retained its original emplacement position (Alapieti, 1982; Järvinen et al., 2020, 2022). In contrast, the Koillismaa Intrusion, emplaced at the boundary between the Archaean basement and the Kuusamo Schist Belt (KSB; Lahtinen & Köykkä, 2020), consists of mafic–ultramafic cumulates and has been tectonically dismembered into east–west-trending blocks (Karinen, 2010). The connecting anomaly has been recognized since the 1950s through ground gravity and airborne geophysical surveys (Salmirinne & Iljina, 2003). Due to its elongated geometry between the exposed intrusions, it was interpreted by Piirainen et al. (1978) and Alapieti (1982) as a potential feeder zone for the magmas of the Koillismaa and Näränkävaara intrusions. This hypothesis was tested

80

85

by GTK through a deep drilling campaign (2020–2021), which confirmed the presence of mafic-ultramafic plutonic rocks at ~1.4 km depth (Karinen et al., 2021; Tirroniemi et al., 2024). The ~300 m thick section intersected by the drillhole represents an unaltered gabbronoritic chilled margin of the Koillismaa Deep Intrusion (KDI; Karinen et al., 2025).

90 The bedrock in the SEEMS DEEP study area is predominantly composed of Archaean orthogneisses. In the southern part of the study area, a narrow belt of banded iron formations (BIFs) is present (Makkonen, 1972), possibly related to the Archaean greenstones located to the east (Järvinen et al., 2023).The region is cross-cut by multiple generations of diabase dykes, likely intruded along pre-existing fractures and faults. Two major shear zones define the structural framework of the area: the N–S-trending dextral Hirvaskoski Shear Zone (HSZ; Kärki & Laajoki, 1995), which marks the western margin of the KSB and
95 separates the Pudasjärvi and Lentua complexes; and the NE–SW-trending sinistral Oulujärvi Shear Zone (OSZ; Kärki & Laajoki, 1995), which intersects the HSZ and passes near the eastern margin of the study area.

3 Seismic response of KLIC and surrounding rocks

3.1 Physical rock properties

The Koillismaa deep drillhole provided critical constraints on the physical rock properties. P-wave velocity measurements
100 were conducted on 1,085 core samples under ambient pressure and temperature conditions, with co-located density measurements (Tirroniemi et al., 2024). These samples were reclassified into 11 main rock types, incorporating lithostratigraphic divisions whenever available. The results are summarized in Figure 2. The overlying basement rocks consist of Archaean gneisses with varying degrees of alteration, leucogranite, granite, and diabase dykes. The median P-wave velocity (Vp) of the basement rocks is approximately 5900 m/s, with values ranging from ~5500 m/s in highly altered gneiss to ~6300
105 m/s in diabase dykes. The upper part of the intrusion includes more felsic lithologies (e.g., granite and quartz diorite dykes) with Vp values around 5900 m/s. The lower, mafic-ultramafic portion comprises gabbronorites (Vp ≈ 6500 m/s), pyroxenites (Vp ≈ 6900 m/s), and peridotites (Vp ≈ 6000 m/s). The relatively low median velocity of peridotites is indicative of serpentinization, however there is no evidence for this process in the drill core. Notably, some highly altered granites with connected porosity exceeding 10% were identified within the intrusion (Bischoff et al., 2024). These rocks exhibit Vp values
110 below 5000 m/s and densities under 2600 kg/m³. The seismic impedance plot (Fig. 2b) suggests that the basement is relatively transparent, with reflections primarily originating from diabase dykes or contacts with highly altered gneisses. In contrast, the mafic-ultramafic rocks exhibit significantly higher acoustic impedance contrast (Zp). Gabbronorites and pyroxenites have Zp values of 19 and 22 ($\times 10^6$ kg·m^{-2}·s^{-1}) respectively, making them strong reflectors, especially at the contacts with felsic rocks. Results from the DAS – VSP survey conducted in the Koillismaa drillhole (Malinowski et al., 2023) confirmed the presence
115 of internal reflections within the KDI. The VSP data also imaged cross-cutting dykes in the basement and responded to intersected faults and major fracture zones.
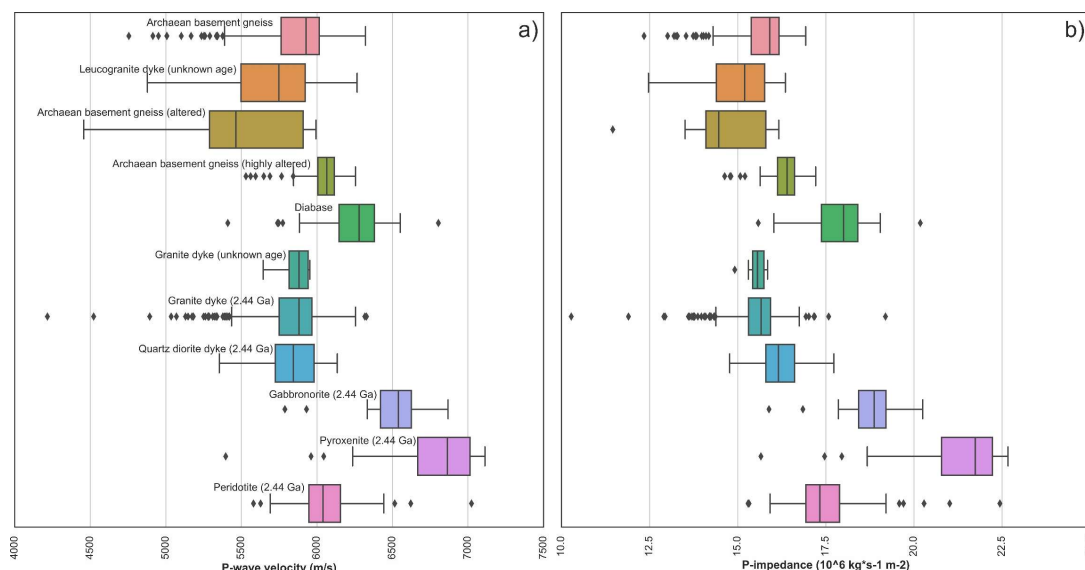
Figure 2: a) Box-and-whisker plot of the measured P-wave velocity using core samples from the Koillismaa deep drillhole grouped
120 **by the rocktype and ordered approximately by depth. The 2.44 Ga age is related to the intrusion. b) Corresponding acoustic**
impedance plot based on the co-located velocity and density measurements.

3.2 Modelling seismic response of KDI as a layered intrusion

The Koillismaa deep drillhole penetrated only the uppermost 300 m of the KDI, whereas gravity data suggest that the intrusion
is significantly thicker (Karinen et al., 2025). The exposed western part of the KLIC, specifically the Koillismaa Intrusion (Fig.

125 1b), reaches thicknesses of up to 2.5 km. To better understand the seismic response of a more complete layered sequence, we
adopted the approach of Deemer and Hurich (1994), who modelled the seismic response of mafic intrusions based on modal
mineralogy. We used a representative stratigraphic section from the Porttivaara block of the Koillismaa Intrusion, where modal
mineralogy was determined from 76 samples (Karinen, 2010). This block comprises a marginal series (MS) up to 200 m thick,
overlain by a layered series (LS). The MS consists of gabbroic cumulates at the base, transitioning upward into more magnesian

130 rocks such as pyroxenites and peridotites. The LS is subdivided into three zones:

- **Lower Zone (LZ)**: olivine gabbronorite (LZa) and gabbronorite (LZb)
- **Middle Zone (MZ)**: a thin basal layer of olivine gabbronorite (MZa), overlain by thick gabbronorite (MZb and MZc),
  separated by subeconomic sulphide mineralization
- **Upper Zone (UZ)**: meso- and leucogabbros (UZa and UZc), with a central oxide gabbro layer (UZb)

135 Elastic properties (Vp, Vs and density) were calculated using the method of Abers and Hacker (2016), based on modal
mineralogy. Assumed mineral compositions included plagioclase (anorthite/albite), orthopyroxene (enstatite 72%, ferrosilite

28%), clinopyroxene (diopside), olivine (forsterite), and brown mica (phlogopite/annite 50:50). Sulphides were replaced by

magnetite. Granophyre was modelled as a mixture of albite (45%), quartz (45%) and biotite (10%). The calculations assumed

emplacement conditions of 15 km depth, 1200°C and 0.4 GPa (Karinen et al., 2025). The resulting elastic properties are shown

140   in Figure 3. Interpolated velocity and density profiles were used to compute a continuous reflection coefficient series in Seismic

Unix (Stockwell, 1999) with frequencies filtered to 62.5 Hz. Prominent reflections correlate with olivine gabbronoritic layers

(LZa and MZc), the sulphide-bearing boundary between MZA and MZb, and the oxide gabbro layer (UZb), which produces

strong top and bottom reflections due to density contrasts. A general increase in seismic velocity and density is observed in

the lowermost 1 km of the section.

145
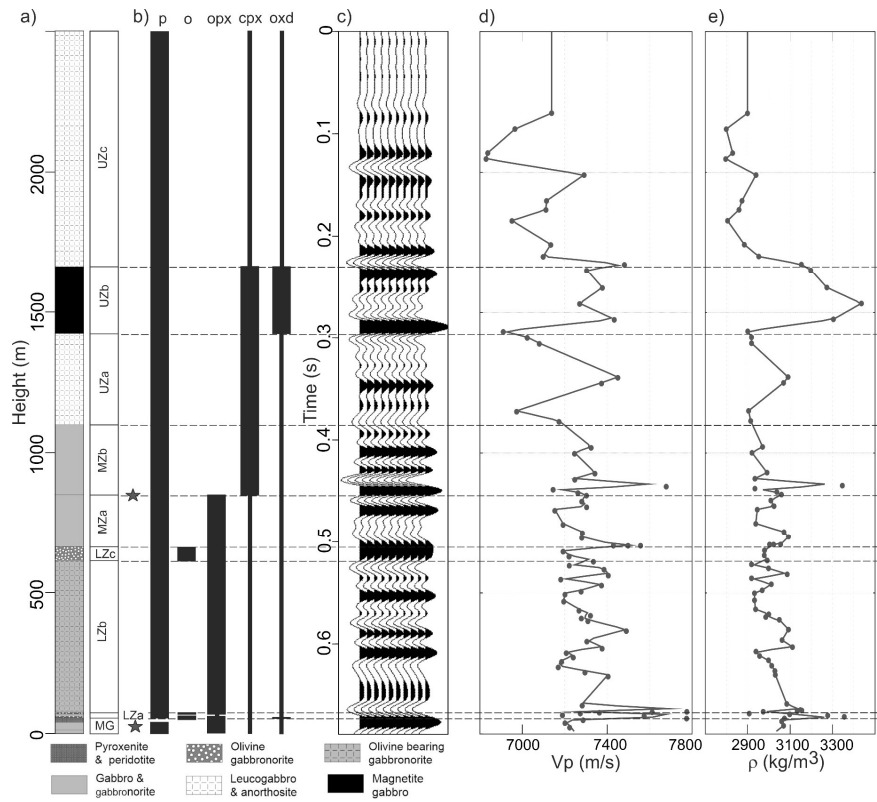
Figure 3: a) Representative stratigraphic section of KLIC based on the profile across the Porttivaara block (Karinen, 2010); b) In the sequence thick vertical lines indicate cumulus minerals and thin vertical lines indicate intercumulus minerals (p-plagioclase, o – olivine, opx – orthopyroxene, cpx – clinopyroxene, oxd – Fe-Ti oxides); stars denote occurrence of sulphide mineralisation (up to 3%); c) corresponding filtered (up to 62.5 Hz) zero-offset reflection coefficient series based on the velocity and density calculated
150   **from modal mineralogy; d) calculated velocity log; e) calculated density log. Points represent samples and the lines are the interpolated values.**

4 Seismic data

4.1 Seismic data acquisition

The 3D seismic survey was conducted in August 2023 in the vicinity of the Koillismaa deep drillhole, approximately 50 km
155   southwest of Kuusamo. The survey area was centered on the gravity anomaly associated with the KDI (Fig. 1b). Terrain
accessibility—characterized by mixed forest, clearings, swamps, and lakes—as well as nature conservation restrictions,
influenced the final layout (Fig. 4a). The eastern boundary of the survey followed the access road to the drill site, which also
hosted one of the 2D profiles (Singh et al., 2025). A large protected swamp area east of this road was excluded from the survey.
The southern extension of the grid was designed to partially cover rocks with strong magnetic signatures (BIFs). The final
160   layout was a compromise between spatial coverage and the number of available receivers (green dots in Fig. 4a). The survey
followed a quasi-orthogonal geometry with 21 receiver lines oriented at an azimuth of 25°N, spaced 240 m apart, covering an
area of ~22 km². A total of 2,866 receivers were deployed at 30 m intervals using nimble nodes equipped with piezoelectric
sensors (Stryde). No prior staking was performed; instead, receivers were planted at pre-plot locations and surveyed using
precision GPS. Additional spikes were attached to nodes to ensure good coupling in swampy areas. Source points were located
165   along forest paths and gravel roads, with a nominal spacing of 30 m (red points in Fig. 4a). Of the 1,615 recorded source points,
718 were located along the two 2D profiles. A Mark IV Vibroseis truck equipped with a Y-2400 Failling shaker (48,000 lbs
peak force) was used as the source, generating 20-second sweeps from 20 – 160 Hz (+1 dB/octave), repeated twice at each
location. The entire 3D survey, including 2D acquisition, was completed in approximately two weeks: ~5 days for node
deployment, ~5 days for production, and ~2.5 days for retrieval.

170

Table 1: Summary of the acquisition parameters of the SEEMS DEEP 3D seismic survey

Acquisition parameters	
Number of live channels	2866 (fixed spread)
Receiver line interval	240 m
Receiver interval	30 m
Receiver type	Piezoelectric (vertical component)
Sampling rate	1 ms
High-cut recording filter	Not applied during data merging
Number of source points	1615
Source interval	30 m
Source type	Vibroseis, 48,000 lbs peak force
Sweep parameters	20-160 Hz, +1dB per octave, 20 s, 75% drive level
Number of sweeps per source point	2
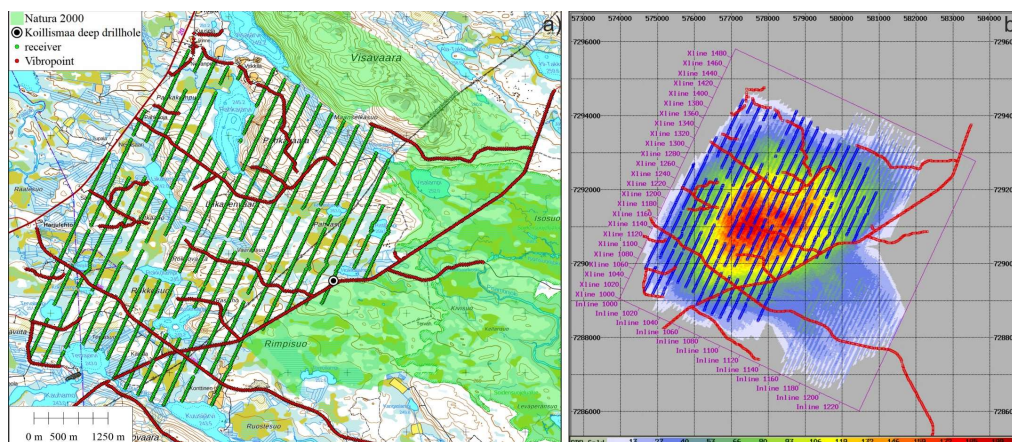
Figure 4: Layout of the SEEMS DEEP 3D seismic survey (a) and the corresponding CDP fold (b).
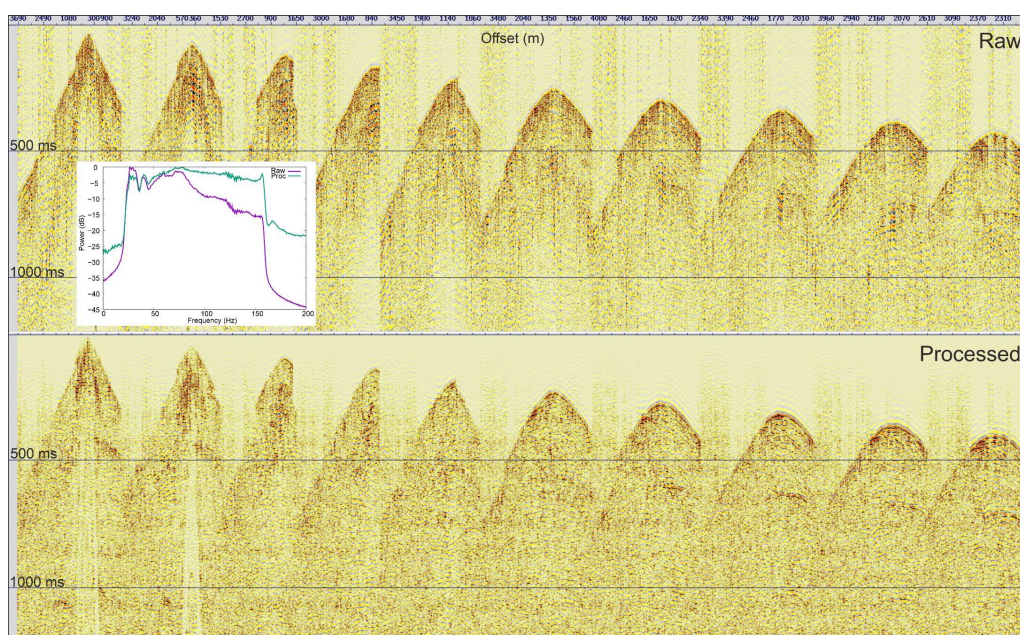
Figure 5: Example of raw (a) and processed (b) shot gather. Inset figure on the top shows the amplitude spectra of raw shot gather (in purple), and after full preprocessing for the same (in green).

This is vibroseis data, I assume that a correlation step is required, correlating the raw recorded traces with the sweep generated by the Vibroseis, I feel if this is correct it should also be comented, was the correlation sweep recorded, extracted from the truck, or was synthetic? (a cople of sentences addressing this issues should be included.

4.2 Seismic data processing and imaging

180   The acquired data were of generally good quality, with clear first arrivals beyond 5 km offset and visible reflections in raw shot gathers (Fig. 5). Low signal-to-noise ratios were observed in swampy areas, particularly in the southern part of the survey. Despite the use of piezoelectric sensors, the data exhibited a broad frequency response consistent with the original sweep (see inset in Fig. 5). The processing workflow followed standard procedures for hardrock seismic data (Table 2). Common depth point (CDP) gathers were generated using a bin size of 15 m (crossline) by 30 m (inline). The inline bin size was increased

185   from 15 m to 30 m to enhance fold, which reached a maximum of 200 in the survey center (Fig. 4b). Refraction statics was derived from approximately 1.9 million auto-picked first arrivals. After testing various algorithms, the best results were

Various algorithms, it might be ilustrative for the reader to know which algoritms were tested as well.

obtained using generalized refraction traveltime inversion (GLI3D; Hampson and Russell, 1984) with a two-layer model. The long-wavelength statics to a floating datum were relatively small, with a bimodal distribution: most values ranged from –6 to 0 ms, and a secondary group from –12 to –6 ms, primarily in the southern part of the survey. Residual refraction statics ranged

190   from –8 to +8 ms. Residual reflection statics were not applied, as they did not significantly improve the stack. Noise attenuation included f–kk filtering, airwave muting, and bandpass filtering. Signal shaping was achieved using spiking deconvolution.

The data were then regularized using 5D interpolation (Trad, 2009), which improved offset-bin distribution and filled data gaps. This step was justified by the presence of laterally coherent reflections with moderate dips. The interpolation used a

195   combination of greedy local Radon transform (Wang et al., 2010), and projection onto convex sets (POCS; Abma and Kabir, 2006), applied in two nested loops along the crossline direction. The interpolation improved reflection continuity in both inline and crossline sections (Fig. 6), particularly near survey edges and in low-fold areas (Fig. 7). Fold increased from ~170 to ~250 in the center and from less than 50 to more than 150 at the edges. However, artifacts were introduced in the top 250 ms of the data, especially in the southeast, and should be interpreted with caution. Can these artifact be identified in the figures, this would be ilustrative for the reader.

200

Following interpolation, several imaging strategies were tested. Pre-stack time migration (PreSTM) yielded the best results compared to post-stack time migration (PoSTM) and dip-moveout (DMO) processing. PreSTM also facilitated velocity picking due to improved signal coherence. Automatic velocity analysis was performed using migrated gathers at every CDP using windowed trace correlations, with a weighted average over 20 inlines and crosslines, and Vrms bounds of 5000 – 6500 m/s.

205   The velocity model was smoothed using a depth-dependent function and refined over two iterations of migration and velocity analysis.

The final PreSTM volume was post-processed using a structure-oriented mean of least variance (MLV) filter (Al-Dossary and Wang, 2012; Schulze and Pearce, 1993), and depth-converted using a constant velocity of 6000 m/s. This value was consistent

210   with the average velocities from the Koillismaa drillhole and provided a good match to the top of the intrusion. Representative inlines and crosslines from the final volume are shown in Figures 8 and 9, with interval velocities overlaid in Figure 10.

Why Pre-stack depth was not used? (a comment indicating why would be ilustrative)

Table 2: Summary of the processing parameters of the SEEMS DEEP 3D seismic survey

Processing parameters	
1. Read data	Correlated shot gathers
2. Vertical stack	Diversity stack
3. Convert to geophone equivalent	Trace integration
4. Resample	2 ms
5. Minimum-phase conversion	Based on theoretical sweep
6. Geometry setup	30/15 m inline/crossline bin width
7. Amplitude recovery	$t^{1.2}$
8. Amplitude scaling	Surface-consistent amplitude scaling
9. Refraction statics	GLI3D, 2 layers, datum = 300 m a.s.l, V_{repl} = 5000 m/s
10. Deconvolution	Single-trace, spiking – 150 ms operator
11. Linear noise removal	*f-kk* filter
12. Airwave attenuation	Median filter
13. Bandpass filtering	Time-variant, 20-30-150-160 Hz to 2 s
14. Amplitude scaling	AGC, 200 ms window
15. Refraction mute	50 ms mute below the predicted first-arrivals
16. 5D interpolation	Crossline direction
17. Pre-stack time migration	Kirchhoff, 2 iterations
18. Automatic velocity analysis	Correlation-based, 2 iterations
19. Gather conditioning	Spectral whitening, Ensemble-amplitude scaling
20. Stack	$1/\sqrt{N}$ normalisation
21. Bandpass filtering	20-30-90-110 Hz
22. Structure-oriented filtering	Mean of least variance (MLV) filter

215
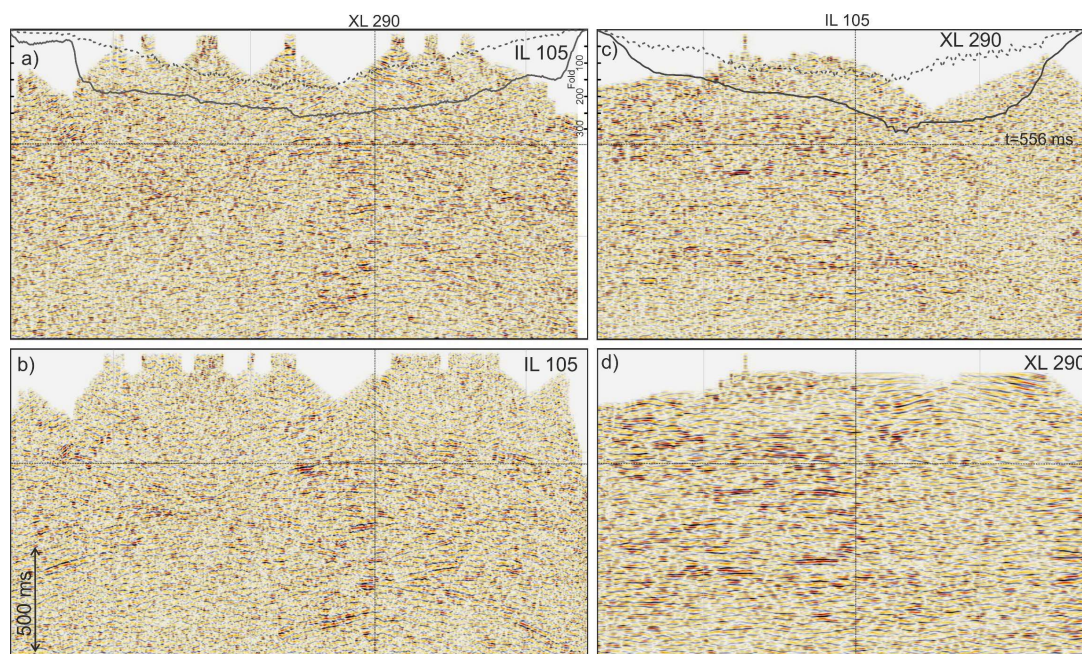
Figure 6: Inline and crossline sections through the stack volumes without (a), (c) and with (b), (d) pre-stack 5D interpolation. Stacking fold is plotted at the top: normal stack - dashed line, interpolated stack – solid line.

220
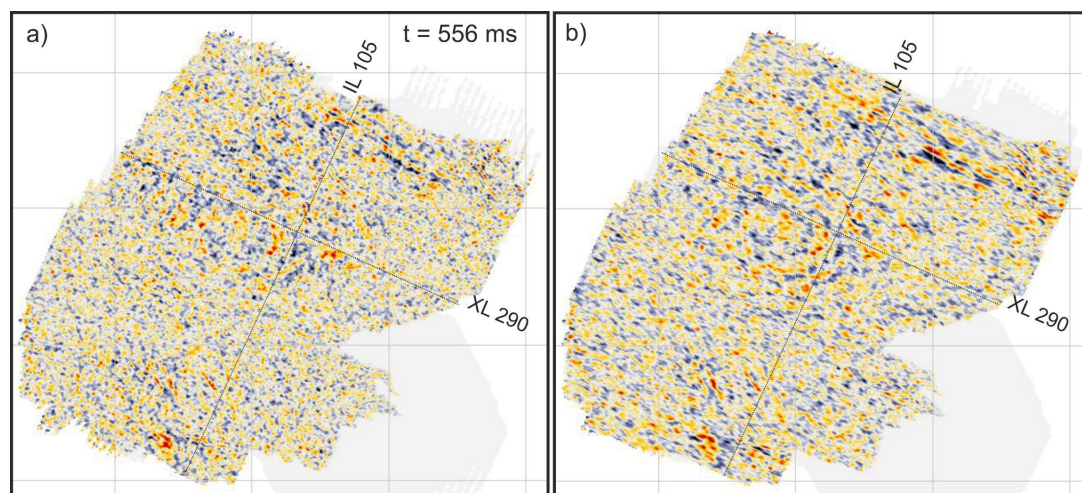
Figure 7: Time slice through the stack volumes without (a) and with (b) pre-stack 5D interpolation.
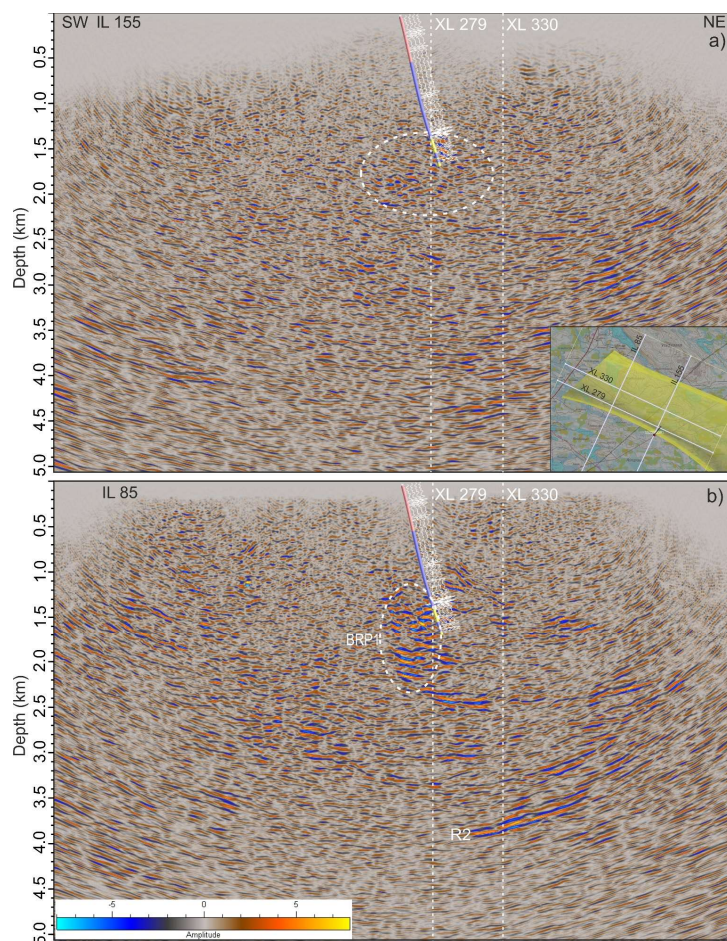
Figure 8: Inline sections from the final PreSTM volume (depth converted). Inset shows location of the sections. Koillismaa drillhole path and simplified lithology (pink - basement, blue - dykes, yellow – intrusion) is shown together with the synthetic seismogram calculated using petrophysical data shown in Fig. 2 and Ormsby wavelet (20-30-90-110 Hz). For labelled reflections see the text.

225
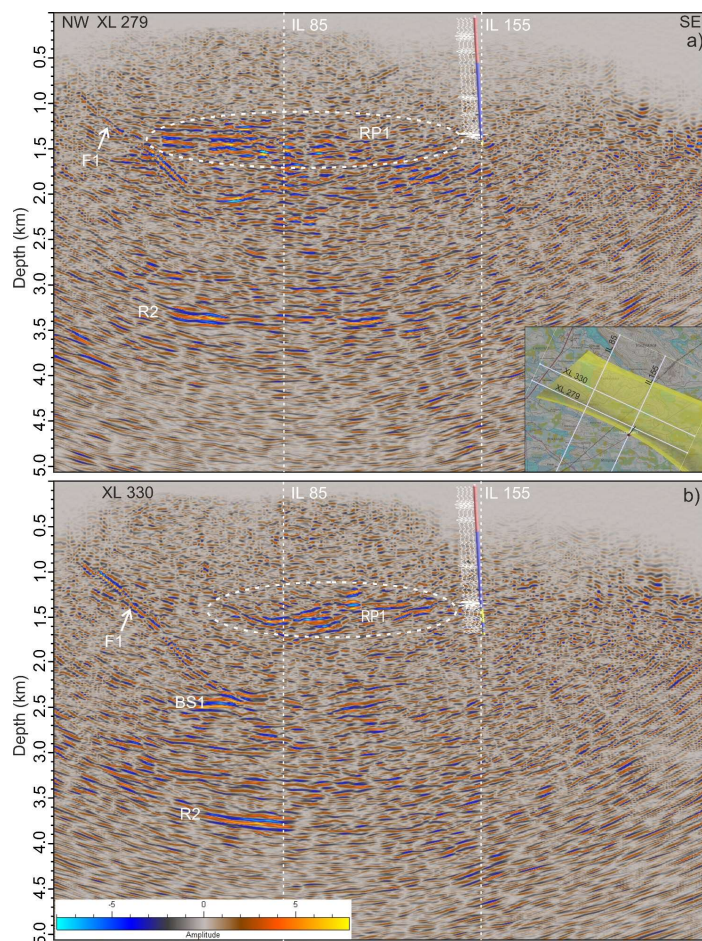
Figure 9: Crossline sections from the final PreSTM volume (depth converted). Inset shows location of the sections. For labelled reflections see the text.
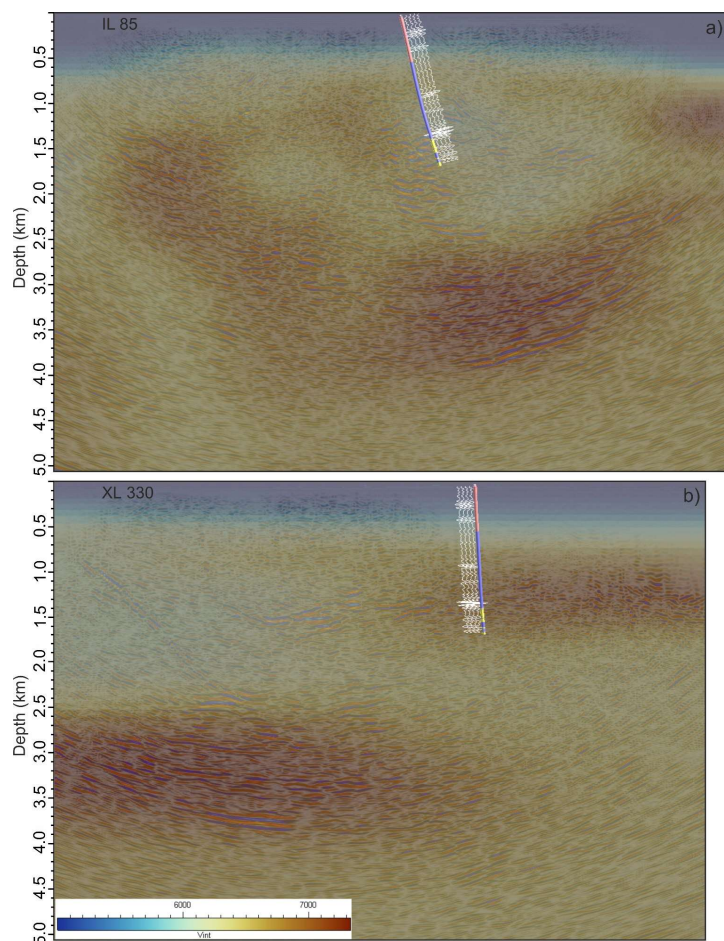
230

Figure 10: Inline 85 and crossline 330 from the final PreSTM volume (depth converted) with the interval velocities in the background.

From the figures presented its difficult to estimate the consistency of the synthetics with the real data, perhaps adding a blow up of the stkaked volume and the synthetics from the interpolated logs would help visualize its consistency.

235

5 Results and interpretation

5.1 General reflectivity characteristics

240   The final PreSTM seismic volume reveals abundant reflectivity, particularly at depths below 1000 m. The most coherent reflections are concentrated in the northeastern part of the survey area. Inline 155 (Fig. 8a) and crossline 279 (Fig. 9a) intersect the Koillismaa drillhole at approximately 1400 m depth. Although reflectivity in this area is somewhat incoherent—likely due to its proximity to the survey edge—an increase in reflectivity is observed where the drillhole intersects the intrusion (1400–

245   1700 m depth), extending to ~2000 m. In contrast, the 2D profile along the access road (Singh et al., 2025) shows more coherent reflections at these depths. Along crossline 279, a ~200 – 300 m thick reflection package (RP1) begins near the drilled top of the intrusion and extends laterally for ~3 km. This package is truncated by a southeast-dipping reflector (F1) at ~45°. Overall, reflections are most abundant between 1400 and 2200 m depth. A strong, subhorizontal reflector (R2) is also observed at ~3300–3400 m depth.

250

Crossline 330 (Fig. 9b), located 780 m northeast of crossline 279, shows an undulating RP1 at ~1400 m depth, underlain by a more transparent zone. Prominent reflections reappear between 2400 – 3400 m. These deeper reflections coincide with high interval velocities (>6600 m/s, locally up to 7300 m/s; Fig. 10b) and terminate at a strong reflector at ~3800 m (R2). Inline 85 (Fig. 8b), located 2130 m northwest of inline 155, shows arcuate reflections between 2400 – 3900 m, with a bottoming point

255   near the drillhole. Some reflectors extend into the southwestern part of the section, where they are associated with higher interval velocities that decrease toward the southwest (Fig. 10a). A prominent, ~600 m wide zone of bright reflectivity (BRP1) is observed southwest of the drillhole between 1400 – 2200 m depth (Fig. 8b). Additional bright spots are present throughout the volume, some near the dipping reflector F1 at depths of ~1400 – 1500 m and ~2000 – 2500 m (e.g., BS1 in Fig. 9b).

5.2 3D seismic interpretation input to the Common Earth Model

260   One of the key objectives of the SEEMS DEEP project was to integrate geophysical and geological data into a Common Earth Model (CEM). Given the sparse geological control, limited to the Koillismaa deep drillhole and a few outcrops, 3D seismic interpretation was essential for constructing the CEM. The model covers a 13 × 13 km (km²) area (Fig. 1b), extending beyond the 3D seismic grid, and incorporates 2D seismic and potential field inversion data. Lithologies in the CEM were simplified into five categories: (1) undifferentiated Archaean basement, (2) banded iron formations (BIFs), (3) felsic (granitic) intrusion

265   envelope, (4) mafic, and (5) ultramafic intrusion components. Snapshots of the CEM along inline 85 and crossline 330 (Fig. 11) show that the intrusion is ~2 – 3 km thick, bounded by distinct reflections (RP1 at the top, R2 at the base). Internal variations in reflectivity and velocity suggest systematic lithological layering, particularly between 2400 – 3400 m depth. These features are interpreted as modal layering or megacyclic units, consistent with the seismic response of the Koillismaa layered series as modelled based on the exposed Porttivara block (Fig. 3c). In the CEM, these are represented by subdividing the intrusion into

270   upper mafic and lower ultramafic units.

The increase in seismic velocity in the lowermost 1000 – 1500 m of the intrusion aligns with predictions based on modal mineralogy (Fig. 3d). The southeast-dipping reflector F1 (Fig. 9) extends to the surface and parallels the Oulujärvi Shear Zone (OSZ), suggesting it is a reverse fault along which the intrusion was thrusted westward (Fig. 10b, 11b). Figure 12 presents westward-oriented views of the CEM. A narrow BIF belt (purple voxels) is associated with a fault system (red surfaces) that

275 parallels the geophysical anomaly between the Koillismaa and Näränkävaara intrusions (Fig. 1b). This interpretation is supported by the presence of sheared BIFs in sparse drillholes south of the study area (Makkonen, 1972). The reverse fault (pale blue surface, Fig. 12c) and the westward-thrust intrusion are also shown.

280
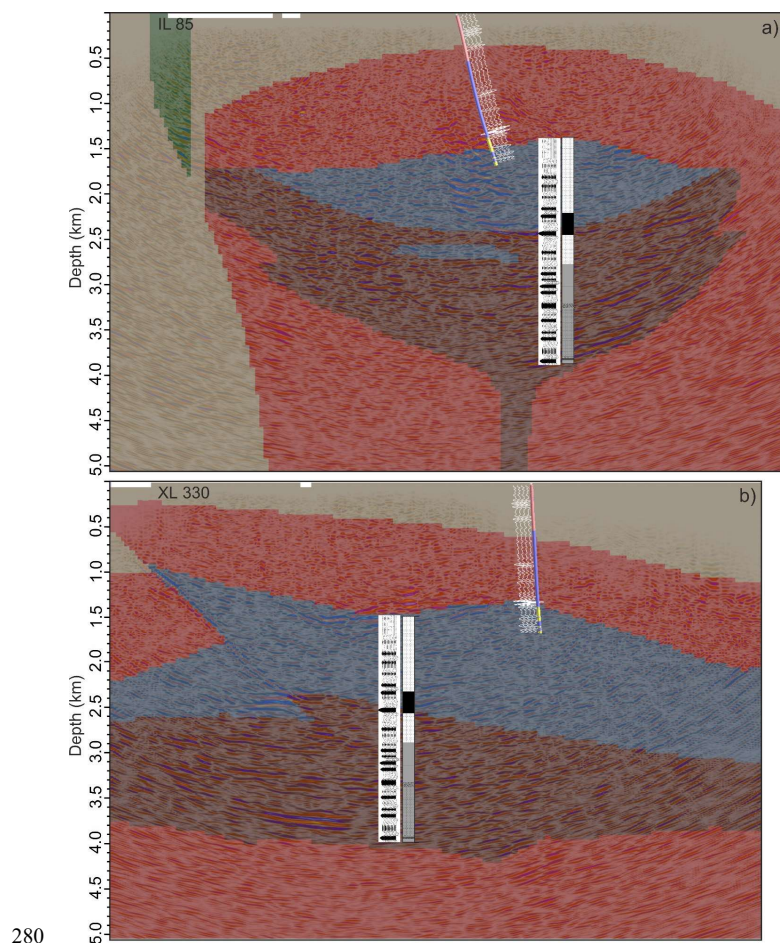
Figure 11: Inline 85 and crossline 330 from the final PreSTM volume (depth converted) with the CEM lithologies in the background. Synthetic seismogram and stratigraphic section from Fig. 3 is also shown for comparison.

285
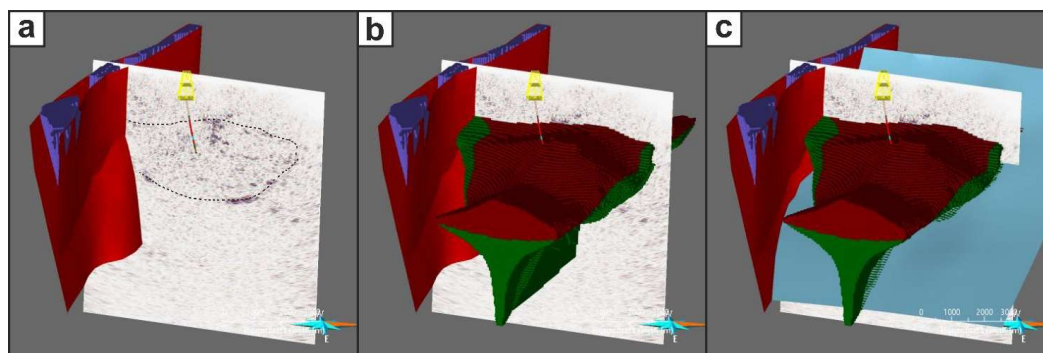
Figure 12: Snapshots of the CEM viewed roughly westward, showing the main lithological units (BIF and intrusion) and associated structures (red and pale blue surfaces). (a) BIF belt (purple) along a fault system (red), (b) voxel model of the intrusion, (c) geometry of the reverse fault (pale blue).
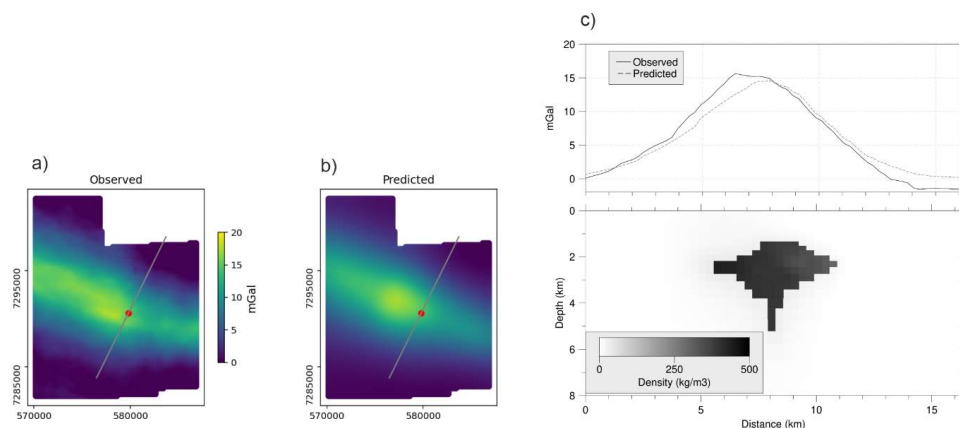
Figure 13: Gravity appraisal of the CEM. Gravity inversion was carried out by allowing density contrast to preferentially only exist within the modelled KDI. (a) Observed, and (b) predicted gravity anomaly. c) Cross-section of the density model and the gravity response along the profile marked with the grey line in (a) and (b). 0 km on the profile represents the southern end of the line. Red dot marks the location of the Koillismaa drillhole.

5.3 Gravity response of the KDI

To validate the CEM, we tested whether it could reproduce the observed gravity anomaly associated with the KDI. A 3D gravity inversion was performed using the jif3D code (Moorkamp et al., 2011), with the constraint that density contrast was allowed only within the mafic-ultramafic intrusion volume. The maximum density contrast was set to 500 kg/m³, consistent with drillhole petrophysical data (Tirroniemi et al., 2024). The inversion began with a uniform density contrast of 0 kg/m³.

305   Cells outside the intrusion were penalized to remain unchanged, and smoothing regularization was disabled at the intrusion boundaries. To account for the mass outside the CEM extent, the KDI was extrapolated northwest and southeast. The input data were residual gravity anomalies derived by removing a regional trend from the Bouguer anomaly (Fig. 1b). The inversion results (Fig. 13) show that the modelled intrusion reproduces the long-wavelength gravity anomaly. The required density contrast approaches the maximum allowed value. A cross-section along a southwest–northeast profile (Fig. 13c) reveals a mass

310   deficit on the southwestern side of the modelled KDI, suggesting either an extension of the intrusion or the presence of other denser rocks (e.g., BIFs).

Format issue: once acronims are defined there is no need to repeat the acronim definitions, with the acronims is enough.

6 Discussion

The 3D seismic data acquired in the SEEMS DEEP project was instrumental in constructing a volumetric model of the Koillismaa Deep Intrusion (KDI) and the broader Common Earth Model (CEM). The internal reflectivity patterns observed in

315   the PreSTM volume — particularly the coherent, laterally continuous reflections suggest that the KDI comprises a thick (2–3 km) layered series at depth. This interpretation aligns with the earlier findings from the 2D seismic studies of the Bjerkreim–Sokndal intrusion (Deemer and Hurich, 1997), where similar reflections were attributed to boundaries between megacyclic circular reasoning, authors are using Deemer & Hurich's work to builld the model. units. Our seismic modelling, based on the modal mineralogy of the western Koillismaa Intrusion, supports the interpretation of the KDI as a more developed, layered intrusion rather than a simple feeder system (see section 3.2). The geometry of the

320   intrusion, as inferred from seismic data, resembles either a tubular (chonolithic) form (Latypov et al., 2024), or a funnel-tube shape (Barnes and Mungall, 2018). Both geometries are thought to evolve from sill-like bodies and have important implications for the localization of mineralization.

Gravity modelling further supports this interpretation. the large scale geometry of the proposed CEM. The inversion results indicate a mass deficit on the southwestern side of

325   the modelled KDI. This could suggest either that the mafic portion of the intrusion extends further west, where seismic reflectivity is less coherent, or that denser rocks are present near the top of the intrusion. The latter possibility is supported by the presence of bright reflectivity zones (e.g., BRP1 in Fig. 8), which may indicate mineralized bodies. A significant outcome of this study is the imaging of a major thrust fault that appears to uplift the northwestern part of the KDI. This structure is not evident in potential field data but is clearly visible in the seismic volume. Its geometry and orientation suggest that it is

330   cogenetic with the Oulujärvi Shear Zone (OSZ), likely formed during the D1 E–W shortening phase of the Svecofennian orogeny (~1.93 – 1.90 Ga; Lahtinen et al., 2023). A similar thrust mechanism may explain the current exposure of the Näränkävaara Intrusion to the east. Moreover, the thrust fault may have acted as a conduit for mineralizing fluids, potentially explaining the bright spot anomalies observed near its trace (e.g., BS1 in Fig. 9b).

335   The SEEMS DEEP 3D seismic survey was executed efficiently, with significant time savings achieved through the use of nimble nodes and stake-less deployment. The nodal system performed well in boreal forest conditions, with no reported issues

in GPS synchronization. For future surveys targeting more complex geology or noisier environments, the high channel count of nodal systems could be further leveraged by reducing receiver spacing. While the 3D data provided high-quality imaging of major structures such as the intrusion and the thrust fault, 2D profiles revealed a greater abundance of shallowly dipping

340 features, interpreted as diabase dykes (Singh et al., 2025). These features are largely absent in the 3D volume, likely due to the relatively sparse acquisition geometry, which limits near-offset coverage. Improved imaging of such features may be achieved through pre-stack depth migration (PSDM) (Singh et al., 2019), coupled with migration velocity analysis (Bräunig et al. 2020, Ziramov et al. 2023) or full-waveform inversion (Singh et al., 2022). These advanced imaging techniques could also help resolve the internal modal layering inferred from the seismic data. Have the authors considered using Fresnel Zone depth maigration?

345   7   Conclusions

The SEEMS DEEP 3D seismic survey has provided unprecedented insight into the deep structure of the Koillismaa Deep Intrusion (KDI), a previously poorly understood segment of the Koillismaa – Näränkävaara Layered Intrusion Complex in northeastern Finland. We employed a cost-effective acquisition strategy using nimble nodes and a single Vibroseis source in combination with the state-of-the art processing techniques e.g., 5D interpolation and automatic velocity analysis. We

350 successfully imaged the subsurface features at depths exceeding 3 km, revealing a complex internal architecture of KDI. Our main findings include: (i) Reinterpretation of the KDI as a more evolved, layered intrusion rather than a simple feeder zone, supported by the coherent reflectivity patterns and seismic velocity contrasts consistent with the modal layering; (ii) Identification of a major thrust fault, likely associated with the Oulujärvi Shear Zone, which appears to have uplifted the northwestern portion of the intrusion. This structure may have played a role in both the emplacement and subsequent

355 deformation of the intrusion; (iii) Integration of geological, seismic, and gravity data into a Common Earth Model (CEM), which successfully reproduces the observed gravity anomaly and provides a volumetric framework for future exploration; (iv) Evidence of potential mineralization zones, inferred from bright reflectivity anomalies and their spatial correlation with structural features   This study demonstrates the feasibility and value of 3D seismic imaging for characterizing layered intrusions in the context of their mineral potential.

360   Data availability

Data associated with this research are available per request to the project coordinator: Uula Autio (uula.autio@gtk.fi), Geological Survey of Finland, Vuorimiehentie 5, 02151 Espoo, Finland.

Team list

Jochen Kamm, Cedric Patzer, Veera Pajunen, Toni Eerola, Tuija Luhta, Viveka Laakso, Olli Salmela (Geological Survey of
365 Finland, GTK); Mathieu Darnet, Francois Bretaudeau, Simon Vedrine, Bitnarae Kim, Florent Beaubois, Jacques Deparis

(French Geological Survey, BRGM); Szymon Oryński (Institute of Geophysics PAS, Poland); Thomas Kalscheuer, Karol Sierszen, Mehrdad Bastani (Uppsala University, Sweden); Catherine Truffert, Fabrice Vermeersch, Julien Gance (IRIS Instruments, France); Marek Wojdyla (Geopartner Geofizyka Sp z o.o., Poland); Antti Kivinen, Janne Kaukolinna (GRM-services Oy, Finland); Yuriy Koltun (Laakso Minerals Oy, Finland).

Author contribution

SH and AG obtained funding. MM, LS, SH, BS, AG designed the 3D survey. LS, MM, BS, AG, SH and UA contributed to the data acquisition. MM performed seismic data processing. UA performed gravity modelling. TK build the geological model. MM, TK and UA interpreted the results. MM wrote the manuscript's main content with major contributions from TK, UA, and other authors. All authors contributed to the final interpretation and discussion of the results.

Competing interests

The contact author has declared that neither they nor their co-authors have competing interests. However, the contact author (MM) is a member of the editorial board of Solid Earth.

Acknowledgments

Thanks to the entire SEEMS DEEP field team for the efforts to acquire the data. Academic licenses of Globe Claritas (PetroSys) and TomoPlus (Geotomo) are acknowledged. Mira Geoscience provided special terms of the Analyst Pro Geophysics software. Structure-oriented filtering of final seismic volumes was performed in OpendTect using Wayne Mogg's plugins (https://github.com/waynegm/OpendTect-Plugins). Seismic Unix was used for generating the synthetic seismograms. Jif3D software package was used for the gravity inversion.

Financial support

SEEMS DEEP is a part of ERA-MIN3 program funded by Business Finland (640/31/2022) (Finland), ANR (ANR-22-MIN3-0006-02) (France), VINNOVA (2022-00209) (Sweden), NCBR (ERAMIN3/1/113/SEEMSDEEP/2022) (Poland).

References

Abers, G. A. and Hacker, B. R.: A MATLAB toolbox and Excel workbook for calculating the densities, seismic wave speeds, and major element composition of minerals and rocks at pressure and temperature, Geochem. Geophys. Geosystems, 17, 616–624, https://doi.org/10.1002/2015GC006171, 2016.

Abma, R. and Kabir, N.: 3D interpolation of irregular data with a POCS algorithm, GEOPHYSICS, 71, E91–E97, https://doi.org/10.1190/1.2356088, 2006.

Alapieti, T.: The Koillismaa layered igneous complex, Finland – its structure, mineralogy and geochemistry, with emphasis on the distribution of chromium, Geol Surv Finland Bull, 319, 1-116, 1982.

395 Alapieti, T. T. and Lahtinen, J. J.: Platinum Group Element Mineralization in the Layered Intrusions of Northern Finland and the Kola Peninsula, Russia. in: The Geology, Geochemistry, Mineralogy and Mineral Beneficiation of Platinum-Group Elements, edited by: Cabri, L. J., Canadian Institute of Mining, Metallurgy and Petroleum, Special Volume 54, 507–546, 2002

Al-Dossary, S. and Wang, Y. E.: Structure-preserving smoothing for 3D seismic attributes, in: SEG Technical Program Expanded Abstracts 2011, 1004–1008, https://doi.org/10.1190/1.3627375, 2012.

400 Autio, U., Darnet, M., Górszczyk, A., Kamm, J., Heinonen, S., Malinowski, M., Kim, B., Singh, B., Vedrine, S., Bretaudeau, F., Patzer, C., Karinen, T., Kalscheuer, T., Truffert, C., Wojdyła, M., Kivinen, A., and Koltun, Y.: Integrating Seismic and Electromagnetic Methods for Deep Mineral Exploration – Results from the SEEMS DEEP Project, 2024, 1–5, https://doi.org/10.3997/2214-4609.202420147, 2024.

Barnes, S. J. and Mungall, J. E.: Blade-shaped dikes and nickel sulfide deposits: a model for the emplacement of ore-bearing
405 small intrusions, Econ. Geol., 113, 789–798, https://doi.org/10.5382/econgeo.2018.4571, 2018.

Bellefleur, G., Schetselaar, E., White, D., Miah, K., and Dueck, P.: 3D seismic imaging of the Lalor volcanogenic massive sulphide deposit, Manitoba, Canada, Geophys. Prospect., 63, 813–832, https://doi.org/10.1111/1365-2478.12236, 2015.

Bischoff, A., Heap, M. J., Mikkola, P., Kuva, J., Reuschlé, T., Jolis, E. M., Engström, J., Reijonen, H., and Leskelä, T.: Hydrothermally altered shear zones: A new reservoir play for the expansion of deep geothermal exploration in crystalline
410 settings, Geothermics, 118, 102895, https://doi.org/10.1016/j.geothermics.2023.102895, 2024.

Bleeker, W., Ernst, R.: Short-lived mantle generated magmatic events and their dyke swarms: The key unlocking Earth's paleogeographic record back to 2.6 Ga, in: Dyke swarms – time markers of crustal evolution, edited by: Hanski, E., Mertanen, S., Rämö, T., Vuollo, J., Taylor & Francis Group, 3–26, 2006.

Bräunig, L., Buske, S., Malehmir, A., Bäckström, E., Schön, M., and Marsden, P.: Seismic depth imaging of iron-oxide
415 deposits and their host rocks in the Ludvika mining area of central Sweden, Geophysical Prospecting, 68, 24–43, https://doi.org/10.1111/1365-2478.12836, 2020.

Ciborowski, T. J. R., Kerr, A. C., Ernst, R. E., McDonald, I., Minifie, M. J., Harlan, S. S., and Millar, I. L.: The Early Proterozoic Matachewan Large Igneous Province: Geochemistry, Petrogenesis, and Implications for Earth Evolution, Journal of Petrology, 56, 1459–1494, https://doi.org/10.1093/petrology/egv038, 2015.

420 Deemer, S. and Hurich, C.: Seismic image of the basal portion of the Bjerkreim-Sokndal layered intrusion, Geology, 25, 1107, https://doi.org/10.1130/0091-7613(1997)025<1107:SIOTBP>2.3.CO;2, 1997.

Deemer, S. J. and Hurich, C. A.: The reflectivity of magmatic underplating using the layered mafic intrusion analog, Tectonophysics, 232, 239–255, https://doi.org/10.1016/0040-1951(94)90087-6, 1994.

Hampson, D. and Russell, B.: First-break interpretation using generalized linear inversion, in: SEG Technical Program
425 Expanded Abstracts 1984, 532–534, https://doi.org/10.1190/1.1894084, 1984.

Heaman, L. M.: Global mafic magmatism at 2.45 Ga: remnants of an ancient large igneous province? Geology, 25, 299-302, https://doi.org/10.1130/0091-7613(1997)025%3C0299:GMMAGR%3E2.3.CO;2, 1997.

Järvinen, V., Halkoaho, T., Konnunaho, J., Heinonen, J. S., Rämö, O. T.: Parental magma, magmatic stratigraphy, and reef-type PGE enrichment of the 2.44-Ga mafic-ultramafic Näränkävaara layered intrusion, Northern Finland, Min Deposita, 55,
430   1535–1560, https://doi.org/10.1007/s00126-019-00934-z, 2020.

Järvinen, V., Halkoaho, T., Konnunaho, J., Heinonen, J. S., Kamo, S., Davey, S., Bleeker, W., Karinen, T., Rämö, O. T.: Petrogenesis of the Paleoproterozoic Näränkävaara layered intrusion, northern Finland, Part II: U-Pb ID-TIMS age and Sm-Nd isotope systematics. Bull Geol Soc Finland, 94, 53–74, https://doi.org/10.17741/bgsf/94.1.003, 2022.

Järvinen, V., Karampelas, N., Rämö, T., Halkoaho, T., Törmänen, T., Mikkola, P., and Lahaye, Y.: Secular change of tectonic
435   setting in the Archean Takanen greenstone belt, northeastern Karelia Province, Fennoscandian Shield, Bulletin of the Geological Society of Finland, 95, 107–134, https://doi.org/10.17741/bgsf/95.2.002, 2023.

Karinen, T.: The Koillismaa Intrusion, northeastern Finland: evidence for PGE reef forming processes in the layered series, Geological Survey of Finland Bulletin, 404, 1-176, 2010.

Karinen, T., Heinonen, S., Konnunaho, J., Salmirinne, H., Lahti, I., Salo A.: Koillismaa Deep Hole – Solving the mystery of
440   a geophysical anomaly, Lithosphere 2021 Symposium, 55–58, 2021.

Karinen. T., Kurhila, M., Moilanen, M., Konnunaho, J., Salmirinne, H., Tirroniemi, J.: Chilled margin and marginal reversal formation in the Koillismaa Deep Intrusion: Implications for parental magma compositions in the 2.44 Ga Tornio–Näränkävaara Belt, Contributions to Mineralogy and Petrology, 2025 (accepted).

Kärki, A. and Laajoki, K.: An interlinked system of folds and ductile shear zones—late stage Svecokarelian deformation in
445   the central Fennoscandian Shield, Finland, Journal of Structural Geology, 17, 1233–1247, https://doi.org/10.1016/0191-8141(95)00006-Y, 1995.

Köykkä, J., Lahtinen, R., Huhma, H.: Provenance evolution of the Paleoproterozoic metasedimentary cover sequences in northern Fennoscandia: Age distribution, geochemistry, and zircon morphology, Precambrian Res, 331, 105364, https://doi.org/10.1016/j.precamres.2019.105364, 2019.

450   Lahtinen, R. and Köykkä, J.: Multiply deformed Paleoproterozoic foreland fold and thrust belt in northern Fennoscandia – The peripheral   Kuusamo   belt   as   a   key   example,   Precambrian   Research,   346,   105825, https://doi.org/10.1016/j.precamres.2020.105825, 2020.

Lahtinen, R., Köykkä, J., Salminen, J., Sayab, M., and Johnston, S. T.: Paleoproterozoic tectonics of Fennoscandia and the birth of Baltica, Earth-Sci. Rev., 246, 104586, https://doi.org/10.1016/j.earscirev.2023.104586, 2023.

455   Latypov, R. M., Namur, O., Bai, Y., Barnes, S. J., Chistyakova, Sy., Holness, M. B., Iacono-Marziano, G., Kruger, W. A. J., O'Driscoll, B., Smith, W. D., Virtanen, V. J., Wang, C. Y., Xing, C.-M., and Charlier, B.: Layered intrusions: Fundamentals, novel   observations   and   concepts,   and   controversial   issues,   Earth-Sci.   Rev.,   249,   104653, https://doi.org/10.1016/j.earscirev.2023.104653, 2024.

Makkonen, V.: Korpuan Jatkotutkimus. Rautaruukki Oy Research Report Ou 16/72, 1972 (in Finnish).

460   Malehmir, A., Juhlin, C., Wijns, C., Urosevic, M., Valasti, P., and Koivisto, E.: 3D reflection seismic imaging for open-pit mine planning and deep exploration in the Kevitsa Ni-Cu-PGE deposit, northern Finland, Geophysics, 77, WC95–WC108, https://doi.org/10.1190/geo2011-0468.1, 2012a.

Malehmir, A., Durrheim, R., Bellefleur, G., Urosevic, M., Juhlin, C., White, D. J., Milkereit, B., and Campbell, G.: Seismic methods in mineral exploration and mine planning: A general overview of past and present case histories and a look into the
465   future, GEOPHYSICS, 77, WC173–WC190, https://doi.org/10.1190/geo2012-0028.1, 2012b.

Malehmir, A., Markovic, M., Marsden, P., Gil, A., Buske, S., Sito, L., Bäckström, E., Sadeghi, M., and Luth, S.: Sparse 3D reflection seismic survey for deep-targeting iron oxide deposits and their host rocks, Ludvika Mines, Sweden, Solid Earth, 12, 483–502, https://doi.org/10.5194/se-12-483-2021, 2021.

Malinowski, M., Brodic, B., Martinkauppi, I., Koskela, E., and Laakso, V.: Distributed acoustic sensing vertical seismic
470   profiling in hardrock environment: case study from Koillismaa drillhole, Finland, 84th EAGE Annual Conference & Exhibition, 1–5, https://doi.org/10.3997/2214-4609.2023101043, 2023.

Manzi, M. S. D., Gibson, M. A. S., Hein, K. A. A., King, N., and Durrheim, R. J.: Application of 3D seismic techniques to evaluate ore resources in the West Wits Line goldfield and portions of the West Rand goldfield, South Africa, GEOPHYSICS, 77, WC163–WC171, https://doi.org/10.1190/geo2012-0133.1, 2012.

475   Moorkamp, M., Heincke, B., Jegen, M., Roberts, A. W., and Hobbs, R. W.: A framework for 3-D joint inversion of MT, gravity and seismic refraction data, Geophys. J. Int., 184, 477–493, https://doi.org/10.1111/j.1365-246X.2010.04856.x, 2011.

Piirainen, T., Hugg, R., Aario, R., Forsström, L., Ruotsalainen, A., Koivumaa, S.: Koillismaan malmikriittisten alueiden tutkimusprojektin loppuraportti 1976. Geol Surv Finland Rep Invest, 18, 51 pp (In Finnish), 1978.

Salmirinne, H. and Iljina, M.: Koillismaan kerrosintruusiokompleksin tulokanavamuodostuman painovoimatulkinta ja alueen
480   malmimahdollisuudet (osa 1). Geol Surv Finland Archive Report Q21/2003/1, 20 pp (In Finnish), 2003.

Schijns, H., Townsend, J., Haddow, D., Shawcross, M., and Ehrig, K.: Sparse 3D seismic survey over the Olympic Dam IOCG deposit, in: Third International Meeting for Applied Geoscience & Energy Expanded Abstracts, International Meeting for Applied Geoscience & Energy, Houston, Texas, 1658–1662, https://doi.org/10.1190/image2023-3908343.1, 2023.

Schulze, M. A. and Pearce, J. A.: Value-and-criterion filters: a new filter structure based on morphological opening and closing,
485   in: Nonlinear Image Processing IV, Backup Publisher: International Society for Optics and Photonics, 106–115, https://doi.org/10.1117/12.144746, 1993.

Singh, B., Malinowski, M., Hloušek, F., Koivisto, E., Heinonen, S., Hellwig, O., Buske, S., Chamarczuk, M., and Juurela, S.: Sparse 3D Seismic Imaging in the Kylylahti Mine Area, Eastern Finland: Comparison of Time Versus Depth Approach, Minerals, 9, https://doi.org/10.3390/min9050305, 2019.

490   Singh, B., Malinowski, M., Górszczyk, A., Malehmir, A., Buske, S., Sito, Ł., and Marsden, P.: 3D high-resolution seismic imaging of the iron oxide deposits in Ludvika (Sweden) using full-waveform inversion and reverse time migration, Solid Earth, 13, 1065–1085, 2022.

Singh, B., Górszczyk, A., Malinowski, M., Heinonen, S., Autio, U., Karinen, T., Wojdyła, M., and SEEMS DEEP Working Group: 2D Seismic Imaging of the Koillismaa Layered Igneous Complex, North-Eastern Finland, EGUsphere, 2025, 1–21,
495   https://doi.org/10.5194/egusphere-2025-496, 2025.

Skyttä, P., Piippo, S., Kloppenburg, A., and Corti, G.: 2. 45 Ga break-up of the Archaean continent in Northern Fennoscandia: Rifting dynamics and the role of inherited structures within the Archaean basement, Precambrian Research, 324, 303–323, https://doi.org/10.1016/j.precamres.2019.02.004, 2019.

Stockwell, J. W.: The CWP/SU: Seismic Un∗x package1,11, Comput. Geosci., 25, 415–419, https://doi.org/10.1016/S0098-3004(98)00145-9, 1999.

Tirroniemi, J., Bischoff, A., Malinowski, M., Autio, U., Karinen, T., Lukkarinen, V., Heinonen, S., Mikkola, P., Leskelä, T., Patzer, C., Piipponen, K., Nousiainen, M., Hakala, P., Martinkauppi, I., Anttilainen, T., Engström, J., Konnunaho, J., Telkkälä, P., and Haavikko, S.: Koillismaa Deep Hole Final Report, GTKn Työraportti - GTK Open File Work Rep., 77, 2024.

Trad, D.: Five-dimensional interpolation: Recovering from acquisition constraints, GEOPHYSICS, 74, V123–V132, https://doi.org/10.1190/1.3245216, 2009.

Wang, J., Ng, M., and Perz, M.: Seismic data interpolation by greedy local Radon transform, GEOPHYSICS, 75, WB225–WB234, https://doi.org/10.1190/1.3484195, 2010.

White, D. J., Secord, D., and Malinowski, M.: 3D seismic imaging of volcanogenic massive sulfide deposits in the Flin Flon mining camp, Canada: Part 1 — Seismic results, GEOPHYSICS, 77, WC47–WC58, https://doi.org/10.1190/geo2011-0487.1, 2012.

White, D. J., Malinowski, M., Devine, C., Gilmore, K., Schetselaar, E., and Pehrsson, S.: Drill Targeting with 3-D Seismics for Volcanogenic Massive Sulfide Exploration in the Flin Flon Mining Camp, Econ. Geol., 111, 903–912, https://doi.org/10.2113/econgeo.111.4.903, 2016.

Yavuz, S., Kinkela, J., Dzunic, A., Penney, M., Neto, R., Araújo, V., Ziramov, S., Pevzner, R., and Urosevic, M.: Physical property analysis and preserved relative amplitude processed seismic imaging of volcanogenic massive sulfides—a case study from Neves–Corvo, Portugal, Geophys. Prospect., 63, 798–812, https://doi.org/10.1111/1365-2478.12269, 2015.

Ziramov, S., Young, C., Kinkela, J., Turner, G., and Urosevic, M.: Pre-stack depth imaging techniques for the delineation of the Carosue Dam gold deposit, Western Australia, Geophys. Prospect., 71, 1077–1095, https://doi.org/10.1111/1365-2478.13314, 2023.